Infrared Physics & Technology 85 (2017) 395–402

Contents lists available at ScienceDirect

Infrared Physics & Technology

journal homepage: www.elsevier.com/locate/infrared

Review

High-efficiency non-uniformity correction for wide dynamic linear infrared radiometry system

Zhou Li [a,b,*], Yi Yu [a], Qi-Jie Tian [a,b], Song-Tao Chang [a], Feng-Yun He [a], Yan-He Yin [a,b], Yan-Feng Qiao [a]

[a] Changchun Institute of Optics, Fine Mechanics and Physics, Chinese Academy of Sciences, Changchun 130033, China
[b] University of Chinese Academy of Sciences, Beijing 100049, China

HIGHLIGHTS

- The calibration formula is employed considering integration time.
- The traditional calibration NUC method for a WDR and CVIT system is analyzed in detail.
- A method is proposed to correct non-uniformity for a WDR and CVIT system.
- Experimental results indicate that the proposed method can fit for wide dynamic range.

ARTICLE INFO

Article history:
Received 24 March 2017
Revised 3 July 2017
Accepted 5 August 2017
Available online 7 August 2017

OCIS:
(010.5630) Radiometry
(040.3060) Infrared
(040.2480) FLIR, Forward-looking infrared
(100.2550) Focal-plane-array image processors

ABSTRACT

Several different integration times are always set for a wide dynamic linear and continuous variable integration time infrared radiometry system, therefore, traditional calibration-based non-uniformity correction (NUC) are usually conducted one by one, and furthermore, several calibration sources required, consequently makes calibration and process of NUC time-consuming. In this paper, the difference of NUC coefficients between different integration times have been discussed, and then a novel NUC method called high-efficiency NUC, which combines the traditional calibration-based non-uniformity correction, has been proposed. It obtains the correction coefficients of all integration times in whole linear dynamic rangesonly by recording three different images of a standard blackbody. Firstly, mathematical procedure of the proposed non-uniformity correction method is validated and then its performance is demonstrated by a 400 mm diameter ground-based infrared radiometry system. Experimental results show that the mean value of Normalized Root Mean Square (NRMS) is reduced from 3.78% to 0.24% by the proposed method. In addition, the results at 4 ms and 70 °C prove that this method has a higher accuracy compared with traditional calibration-based NUC. In the meantime, at other integration time and temperature there is still a good correction effect. Moreover, it greatly reduces the number of correction time and temperature sampling point, and is characterized by good real-time performance and suitable for field measurement.

Contents

* Corresponding author at: Changchun Institute of Optics, Fine Mechanics and Physics, Chinese Academy of Sciences, Changchun 130033, China.
E-mail address: lizhou13mails@sina.com (Z. Li).

http://dx.doi.org/10.1016/j.infrared.2017.08.004
1350-4495/

1. Introduction

Currently, ground-based infrared imaging systems are widely used to measure radiometric characteristics of military and scientific objects. In infrared radiometry systems, the infrared focal plane array (IRFPA) is one of the most important components. However, restricted by the level of immature manufacturing crafts, the infrared focal plane array is still troubled with a phenomenon of non-uniformity [1–3]. Non-uniformity is attributable to the different photo response of each pixel when they receive the same infrared radiation. Consequently, the existence of non-uniformity would degrade radiometry precision and imaging quality seriously [4]. Hence, non-uniformity correction (NUC) is an essential part of the metrology and calibration of infrared radiometric systems [5,6]. For an infrared radiometry system, the cause of non-uniformity primarily comes from two aspects: (1) one is the detector itself [7]; (2) the other is the optical system including the radiation emitted by lens, lens alignment, vignetting effect and so on. Especially, the latter is sensitive to fluctuation of ambient temperature [8]. Therefore, NUC is reconsidered to conduct periodically [9]. To compensate and remedy the non-uniformity, various methods have been proposed. In general, two main kinds of NUC methods have been developed, namely the scene-based NUC method and the calibration-based NUC method [10,11]. As the most effective and reliable method, the calibration-based NUC method employs a standard reference as the calibration source to calculate the correction parameters [12]. The benefits of this method lie in its simplicity and low computational complexity. The trouble of this method is that the non-uniformity is not stationary and slowly drifts with time, therefore a periodic update of NUC is required [13,14]. Compared with the calibration-based NUC method, the scene-based NUC method only relies on the information of the imaging scene, reducing the operation complexity and imaging interruption [15,16]. Unfortunately, most of them still suffer from artificial ghosting, computational complexity and image blurring [17,18].

So far, with the rapid progress of technology, a variety of supersonic missiles and aircrafts emerge. If targets with such characteristics are observed and tracked, an infrared radiometry system with Wide Dynamic Range (WDR) and Continuous Variable Integration Time (CVIT) would be required to get more information of the target [19]. As a consequence, it is of significance and prospect for an infrared system supported with WDR and CVIT [7,20]. Considering the good performance of cooled IRFPAs, most of ground-based infrared radiometry systems are usually characteristic of a wide linear dynamic range. The so-called wide linear dynamic range refers to that infrared radiometric systems can effectively accommodate from small to large scale radiance with a linear response. In outfield, the infrared radiometry systems generally image and measure targets at low or high temperatures by switching integration time. Due to the high accuracy of military radiometry and observation, the calibration-based NUC method would have been employed for ground-based infrared radiometry systems [21]. According to the modulation of different parameters, the calibration-based NUC method is generally classified as the blackbody-based non-uniformity correction (BBNUC) method and the integration-based non-uniformity correction (IBNUC) method [22]. For BBNUC method, the coefficients of BBNUC need to be recalculated one by one at each integration time. As for IBNUC method, it is valid only if the temperature of target consistent with the standard reference utilized in NUC [23]. Obviously, that is so harsh and flexible-less which makes them limitative in complex outfield. Considering that, a high-efficiency NUC method has been put forward in this paper.

In the following, the calibration considering integration time was adopted for the wide dynamic system and two calibration-based NUC methods – BBNUC and IBNUC – respectively applicable for WDR and CVIT infrared radiometry systems were analyzed in Section 2. After that, a novel solution based on calibration-based NUC method called high-efficiency NUC method specialized for the WDR and CVIT infrared radiometric system was proposed in Section 3. In Section 4, the experiments on calibration and NUC were carried out based on a diameter of 400 mm ground-based infrared radiometry system. It was concluded in Section 5 that our method yields high accuracy for a WDR and CVIT infrared radiometry system. Besides, it has better performance in efficiency and time consumption and provides users with a feasible NUC method in outfield.

2. Model of radiometric calibration and calibration-based NUC theory

2.1. Calibration considering the integration time

The cooled infrared pixels are operated with fine linear input-output characteristics in many realistic applications. In this paper, radiometric calibration formulas considering the integration time are adopted. Multiple integration times are usually introduced for WDR systems. The output gray value $I_{i,j}(t, T_{Bb})$ is given by the approximate linear relation [24]:

$$I_{i,j}(t, T_{Bb}) = t \cdot (R_{i,j} \cdot L(T_{Bb}) + I_{i,j}^{(\text{stray})}) + I_{i,j}^{(\text{dark})}, \tag{1}$$

where $I_{i,j}(t, T_{Bb})$ is the gray value of the (i,j)th pixel in the array, t is the integration time in units of milliseconds, T_{Bb} is the temperature of blackbody, $L(T_{Bb})$ is the radiance of an ideal blackbody. $R_{i,j}$ is the normalized radiation flux response, $I_{i,j}^{(\text{stray})}$ is the offset caused by

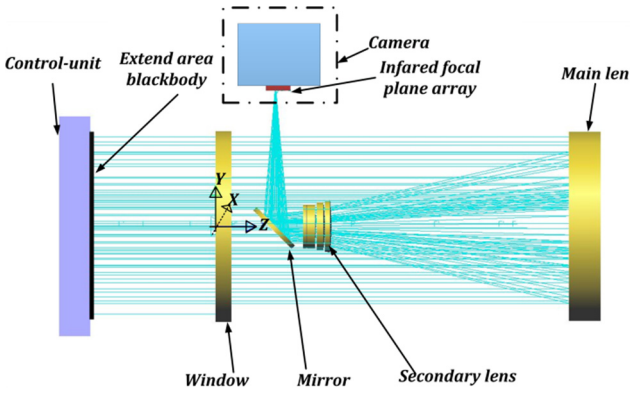

Fig. 1. Schematics diagram of radiometric calibration based on an extended standard blackbody.

ambient temperature and $I_{i,j}^{(\mathrm{dark})}$ is the offset caused by internal factors [25].

In the Eq. (1), it illustrates the linear relationship between the output of gray value and the integration time, the radiance of the target. To calibrate an infrared radiometry system, the near extend homogeneous source method is usually employed at preselected integration time. An extended standard blackbody is placed near the entrance pupil of an infrared system. This method yields high calibration accuracy because the atmospheric effects such as absorption and scattering can be ignored. The schematics diagram of calibration is illustrated in Fig. 1 [26].

2.2. The blackbody-based NUC method for wide dynamic range infrared radiometry systems

The blackbody-based non-uniformity correction (BBNUC) is one of the most simple and effective NUC methods for infrared radiometry systems, which obtains different temperatures of reference source with a fixed integration time. To be specific, an average of 20 frames generally is collected to reduce the effect of stochastic noise. Supposing that the integration time is t_0, the temperatures of blackbody are set T_l and T_h, respectively. According to Eq. (1) [27]:

$$\begin{cases} I_{i,j}(t_0,T_l) = \mathrm{t}_0 \cdot R_{i,j} \cdot L(T_l) + \mathrm{t}_0 \cdot I_{i,j}^{(\mathrm{stray})} + I_{i,j}^{(\mathrm{dark})} \\ I_{i,j}(t_0,T_h) = \mathrm{t}_0 \cdot R_{i,j} \cdot L(T_h) + \mathrm{t}_0 \cdot I_{i,j}^{(\mathrm{stray})} + I_{i,j}^{(\mathrm{dark})} \end{cases}. \tag{2}$$

Assuming that the number of pixels is M×N, so the average gray value $\overline{I(t_0,T_l)}$,$\overline{I(t_0,T_h)}$ at low temperature T_l and high temperature T_h could be separately calculated by:

$$\begin{cases} \overline{I(t_0,T_l)} = \frac{\sum_{i=1}^{\mathrm{M}}\sum_{j=1}^{\mathrm{N}} I_{i,j}(t_0,T_l)}{\mathrm{M}\times\mathrm{N}} \\ \overline{I(t_0,T_h)} = \frac{\sum_{i=1}^{\mathrm{M}}\sum_{j=1}^{\mathrm{N}} I_{i,j}(t_0,T_h)}{\mathrm{M}\times\mathrm{N}} \end{cases}. \tag{3}$$

The coefficients $K_{i,j}^{(\mathrm{bb})}(t_0,T)$ and $B_{i,j}^{(bb)}(\mathrm{t}_0,T)$ based on BBNUC method can be expressed as:

$$\begin{cases} K_{i,j}^{(\mathrm{bb})}(t_0,T) = \frac{\overline{I(t_0,T_h)}-\overline{I(t_0,T_l)}}{I_{i,j}(t_0,T_h)-I_{i,j}(t_0,T_l)} \\ B_{i,j}^{(bb)}(t_0,T) = \overline{I(t_0,T_h)} - K_{i,j}^{(\mathrm{bb})}(\mathrm{t}_0,T)\cdot I_{i,j}(t_0,T_h) \end{cases}. \tag{4}$$

Now suppose that the blackbody's temperature is still T and then turn the integration time from t_0 to t. That is to say we correct $I_{i,j}(t,T)$ at any integration time and temperature by Eq. (4). The corrected output response $I_{i,j}^{(\mathrm{c})}(t,T)$ by BBNUC method could be described as follows:

$$\begin{aligned} I_{i,j}^{(\mathrm{c})}(t,T) &= K_{i,j}^{(\mathrm{bb})}(\mathrm{t}_0,T)\cdot I_{i,j}(t,T) + B_{i,j}^{(\mathrm{bb})}(\mathrm{t}_0,T) \\ &= \mathrm{t}\cdot R_{i,j}\cdot L(T) + (\mathrm{t}-\mathrm{t}_0)\cdot\frac{\overline{R}}{R_{i,j}}\cdot I_{i,j}^{(\mathrm{stray})} + \mathrm{t}_0\cdot\overline{I^{(\mathrm{stray})}} + \overline{I^{(\mathrm{dark})}} \end{aligned} \tag{5}$$

where $\overline{R}$ is the average flux response for all pixels of the detector at the corresponding temperature and integration time, $\overline{I^{(\mathrm{stray})}}$ is the average gray value of entire detector introduced by the external environment, $\overline{I^{(\mathrm{dark})}}$ is the average gray value produced by internal factors of the detector.

The corrected error $\Delta I(t,T)$ is defined as follows:

$$\Delta I(t,T) = I_{i,j}^{(c)}(t,T) - \overline{I(t,T)} = (\mathrm{t}-\mathrm{t}_0)\cdot\overline{R}\cdot(L_{i,j}^{(\mathrm{stray})} - \overline{L^{(\mathrm{stray})}}). \tag{6}$$

where $\overline{I(t,T)}$ is the average gray value of detector at the integration time t and the temperature T. $L_{i,j}^{(\mathrm{stray})}$ is the radiance of stray radiation corresponding to pixel (i,j). $\overline{L^{(\mathrm{stray})}}$ is the average radiance emitted by the external ambient. For the BBNUC method, ignoring the effect of nonlinearity and stochastic noise, we get $I_{i,j}^{(\mathrm{c})}(t,T) = \overline{I(t,T)}$, which means that the correction error of BBNUC is zero in theory [28]. However, considering the factors such as alignment of lens, cold reflection and stray radiation, it can hardly guarantee the corrected error $\Delta I(t,T) = 0$, especially when regarding a large-diameter infrared radiometry system. The NUC for random integration time couldn't be replaced by the coefficients of BBNUC at a fixed integration time, which suffers from such errors. That is why we have to correct one by one at all integration times. The annoyance is excessive time for NUC and frequent interruption tasks, which is clearly intolerable during the process of mission.

2.3. The integration-based NUC method for wide dynamic range infrared radiometry systems

The integration-based non-uniformity correction (IBNUC) method, as one of calibration-based NUC methods, mainly adopts two integration times (t_s and t_l, $t_s < t_l$) and a fixed temperature to conduct NUC. This method is suitable for situations that the source's temperature remains constant or changes slightly.The coefficients of IBNUC method can be calculated similar to BBNUC method. Assuming that temperature of the radiant source is T_0. The coefficients $K_{i,j}^{(\mathrm{int})}(t_0,T)$ and $B_{i,j}^{(\mathrm{int})}(\mathrm{t}_0,T)$ based on IBNUC method can be given as follows:

$$\begin{cases} K_{i,j}^{(\mathrm{int})}(t,\mathrm{T}_0) = \frac{\overline{I(t_l,T_0)}-\overline{I(t_s,T_0)}}{I_{i,j}(t_l,T_0)-I_{i,j}(t_s,T_0)} \\ B_{i,j}^{(\mathrm{int})}(t,T_0) = \overline{I(t_l,T_0)} - K_{i,j}^{(\mathrm{int})}\cdot(t,T_0)\cdot I_{i,j}(t_l,T_0) \end{cases}. \tag{7}$$

where the average gray value $\overline{I(t_l,T_0)}$ and $\overline{I(t_s,T_0)}$ are respectively obtain at long integration time t_l and short integration time t_s.

When the temperature is set as T, the integration time is given as t, the output gray value of pixel can be expressed as Eq. (1). Similarly, if the parameters acquired at T_0 are still employed, the corrected output response $I_{i,j}^{(\mathrm{c})}(t,T)$ can be expressed as follows:

$$\begin{aligned} I_{i,j}^{(\mathrm{c})}(t,\mathrm{T}) &= K_{i,j}^{(\mathrm{int})}\cdot(t,T_0)\cdot I_{i,j}(t,T) + B_{i,j}^{(\mathrm{int})}(t,T_0) \\ &= t\cdot\frac{\overline{R}\cdot L(T_0)+\overline{I^{(\mathrm{stray})}}}{R_{i,j}\cdot L(T_0)+I_{i,j}^{(\mathrm{stray})}}\cdot[R_{i,j}\cdot L(T) + I_{i,j}^{(\mathrm{stray})}] + \overline{I^{(\mathrm{dark})}}. \end{aligned} \tag{8}$$

The correction error $\Delta I(t,T)$ is defined as follows:

$$\begin{aligned} \Delta I(t,T) &= I_{i,j}^{(\mathrm{c})}(t,\mathrm{T}) - \overline{I(t,\mathrm{T})} \\ &= t\cdot\left(\frac{\overline{R}\cdot I_{i,j}^{(\mathrm{stray})} - R_{i,j}\cdot\overline{I^{(\mathrm{stray})}}}{R_{i,j}\cdot L(T_0)+I_{i,j}^{(\mathrm{stray})}}\right)\cdot(L(T_0)-L(T)). \end{aligned} \tag{9}$$

where $L(T_0)$ is the radiance at temperature T_0, $L(T)$ is the radiance of an ideal blackbody at temperature T.

In the same way, if we don't consider the factor of nonlinearity and stochastic noise, there would be $I_{i,j}^{(\mathrm{c})}(t,T) = \overline{I(t,T)}$. But the scene usually changes ($L(T)\neq L(T_0)$), the uniformity will deteriorate. It's denominated that the IBNUC method is also not suitable for a wide dynamic range infrared radiometry system.

3. High-efficiency non-uniformity correction

In practice, the output gray value should be neither too low nor too high when operating radiometry. Because low gray value leads to poor noise-to-signal ratio, while a saturated gray value makes radiometry invalid. It's usually between 30% and 70% in linear region of infrared detectors. That makes many problems brief and convenient especially for NUC and radiometry. At present, we emphasize that although BBNUC method is simple and accurate, it's required to correct one by one at all integration times during one mission, which suffers from the consequence of huge

workload and time-consuming; for IBNUC method, the condition that a minimal disparity of temperature between the target and the reference is required, thus it can hardly adjust to the complex outfield apparently.

Combining the advantages of the two calibration-based NUC methods described above, an efficient and real-time solution method called high-efficiency NUC has been put forward for a WDR and CVIT system. In this method it simply requires three different images, two different temperatures T_l and T_h, two integration times t_s and t_l included in these images. The specific procedure is as follows:

- Set the integration time t_s and the temperature of blackbody T_l separately, take image $I_1(t_s, T_l)$.
- Remain the blackbody's temperature constant; turn the integration from t_s to t_l, gain image $I_2(t_l, T_l)$.
- The integration time constant and transfer the temperature from T_l to T_h, obtain image $I_3(t_l, T_h)$.

According to the images $I_1(t_s, T_l)$, $I_2(t_l, T_l)$ and $I_3(t_l, T_h)$, the coefficients $K_{i,j}^{(\mathrm{int})}(t, \mathrm{T_l})$, $B_{i,j}^{(\mathrm{int})}(t, \mathrm{T_l})$, $K_{i,j}^{(\mathrm{bb})}(\mathrm{t_l}, T)$ and $B_{i,j}^{(\mathrm{bb})}(\mathrm{t_l}, T)$ could be inferred. Based on the explanations above, the parameters of high-efficiency NUC can be described as follows.

The corrected output $I^{(c)}(\mathrm{t_l}, T)$ by BBNUC method,

$$\begin{aligned} I^{(c)}(\mathrm{t_l}, T) &= K_{i,j}^{(\mathrm{bb})}(\mathrm{t_l}, T) \cdot I_{i,j}(\mathrm{t_l}, T) + B_{i,j}^{(\mathrm{bb})}(\mathrm{t_l}, T) \\ &= K_{i,j}^{(\mathrm{bb})}(\mathrm{t_l}, T) \cdot (t_l \cdot R_{i,j} \cdot L(T) + \mathrm{t_l} \cdot I_{i,j}^{(\mathrm{stray})} + I_{i,j}^{(\mathrm{dark})}) \\ &\quad + B_{i,j}^{(\mathrm{bb})}(\mathrm{t_l}, T). \end{aligned} \tag{10}$$

For the whole detector, the calibration equation should be satisfied:

$$\overline{I(\mathrm{t_l}, T)} = \mathrm{t_l} \cdot \overline{R} \cdot L(T) + \mathrm{t_l} \cdot \overline{I^{(\mathrm{stray})}} + \overline{I^{(\mathrm{dark})}}. \tag{11}$$

By Eqs. (10) and (11):

$$\mathrm{t_l} \cdot \overline{I^{(\mathrm{stray})}} + \overline{I^{(\mathrm{dark})}} = K_{i,j}^{(\mathrm{bb})}(\mathrm{t_l}, T) \cdot [\mathrm{t_l} \cdot I_{i,j}^{(stray)} + I_{i,j}^{(\mathrm{dark})}] + B_{i,j}^{(\mathrm{bb})}(\mathrm{t_l}, T). \tag{12}$$

On the other hand, $I^{(c)}(\mathrm{t_l}, T)$ by IBNUC method:

$$I^{(c)}(t, T_l) = K_{i,j}^{(int)}(t, T_l) \cdot I(t, T_l) + B_{i,j}^{(int)}(t, T_l). \tag{13}$$

Similarly, for the entire detectors, for random integration time t, it should satisfy:

$$\overline{I(t, T_l)} = t \cdot \overline{(R_{i,j} \cdot L(T_l) \cdot I_{i,j}^{(stray)})} + \overline{I^{(dark)}}. \tag{14}$$

From Eqs. (13) and (14):

$$\overline{I^{(\mathrm{dark})}} = K_{i,j}^{(\mathrm{int})}(t, \mathrm{T_l}) \cdot I_{i,j}^{(\mathrm{dark})} + B_{i,j}^{(\mathrm{int})}(t, \mathrm{T_l}). \tag{15}$$

For random integration time t, temperature $\mathrm{T_l}$, the result by BBNUC method can be expressed as:

$$\begin{aligned} I^{(\mathrm{c})}(\mathrm{t}, T_l) &= K_{i,j}^{(\mathrm{bb})}(\mathrm{t}, T_l) \cdot I_{i,j}(t, \mathrm{T_l}) + B_{i,j}^{(\mathrm{bb})}(\mathrm{t}, T_l) \\ &= K_{i,j}^{(\mathrm{bb})}(\mathrm{t}, T_l) \cdot [\mathrm{t} \cdot R_{i,j} \cdot L(T_l) + t \cdot I_{i,j}^{(\mathrm{stray})} + I_{i,j}^{(\mathrm{dark})}] \\ &\quad + B_{i,j}^{(\mathrm{bb})}(\mathrm{t}, T_l). \end{aligned} \tag{16}$$

$$\overline{I(t, \mathrm{T_l})} = t \cdot \overline{R} \cdot L(T_l) + t \cdot \overline{I^{(\mathrm{stray})}} + \overline{I^{(\mathrm{dark})}} \tag{17}$$

For BBNUC, the temperature could be adjustable, but there are the same coefficients of NUC:

$$B_{i,j}^{(\mathrm{bb})}(\mathrm{t}, T_l) = B_{i,j}^{(\mathrm{bb})}(\mathrm{t}, T) \tag{18}$$

From Eqs. (16)(18):

$$t \cdot \overline{I^{(\mathrm{stray})}} + \overline{I^{(\mathrm{dark})}} = K_{i,j}^{(\mathrm{bb})}(t, \mathrm{T_l}) \cdot [t \cdot I_{i,j}^{(\mathrm{stray})} + I_{i,j}^{(\mathrm{dark})}] + B_{i,j}(t, \mathrm{T}). \tag{19}$$

In short:

$$\begin{cases} \overline{I^{(\mathrm{stray})}} = K_{i,j}(t, T) \cdot I_{i,j}^{(\mathrm{stray})}(t, T) + \frac{B_{i,j}^{(\mathrm{bb})}(\mathrm{t_l}, T) - B_{i,j}(t, T)}{t_h - t} \\ \overline{I^{(\mathrm{dark})}} = K_{i,j}^{(\mathrm{int})}(t, \mathrm{T_l}) \cdot I_{i,j}^{(\mathrm{dark})} + B_{i,j}^{(\mathrm{int})}(t, \mathrm{T_l}) \end{cases}. \tag{20}$$

$$B_{i,j}(t, T) = \frac{\mathrm{t_l} - t}{\mathrm{t_l}} \cdot B_{i,j}^{(\mathrm{int})}(t, \mathrm{T_l}) + \frac{t}{t_l} \cdot B_{i,j}^{(\mathrm{bb})}(\mathrm{t_l}, T). \tag{21}$$

At last, we get the parameter:

$$\begin{cases} K_{i,j}(t, T) = K_{i,j}^{(\mathrm{bb})}(\mathrm{t_l}, T) \\ B_{i,j}(t, T) = \frac{\mathrm{t_l} - t}{\mathrm{t_l}} \cdot B_{i,j}^{(\mathrm{int})}(t, \mathrm{T_l}) + \frac{t}{\mathrm{t_l}} \cdot B_{i,j}^{(\mathrm{bb})}(\mathrm{t_l}, T) \end{cases} \tag{22}$$

The NUC coefficients of random integration time can be obtained effectively from Eq. (22). From the equations above, we can see that the high-efficiency method simply requires three different images involving two different temperatures and two different integration time points. For a system with WDR and CVIT, the high-efficiency method save the required time and cut down the cost, while the traditional NUC always interrupts the assignment to conduct the NUC.

4. Experimental results

4.1. Experimental setup

To verify the model of calibration considering integration time and high-efficiency NUC method described above, the experiments were performed on a mid-wave infrared (MWIR) system having a large-scale infrared focal plane array (320 × 256 pixels). The system has a diameter of 400 mm and a focal length of 800 mm. The infrared focal plane array operates in 0.8–2.5 μm waveband, with a 14-bit digital output. The size of pixel is 30 μm × 30 μm.

The SR800 extended area blackbody manufactured by CI systems is adopted to calibrate the MWIR system. The blackbody has a 20 × 20 in. (500 × 500 mm) size and exhibits high emissivity (0.97 in 3–5 μm waveband). The temperature accuracy is 0.1 °C over an operating temperature range of 5–150 °C. The experimental set-up used for radiometric calibration and measurement is shown in Fig. 2.

4.2. Verification of linear response

To verify the relationship between the output gray value and the radiance as well as the integration time, experiment of

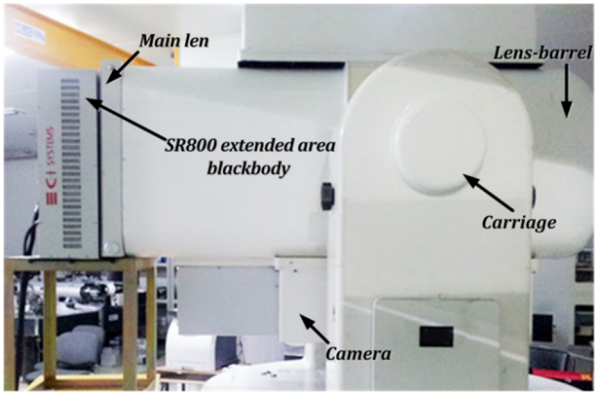

Fig. 2. Setup of Φ400 mm infrared radiometry system and 20 × 20 in. extended area blackbody for radiometric calibration and NUC.

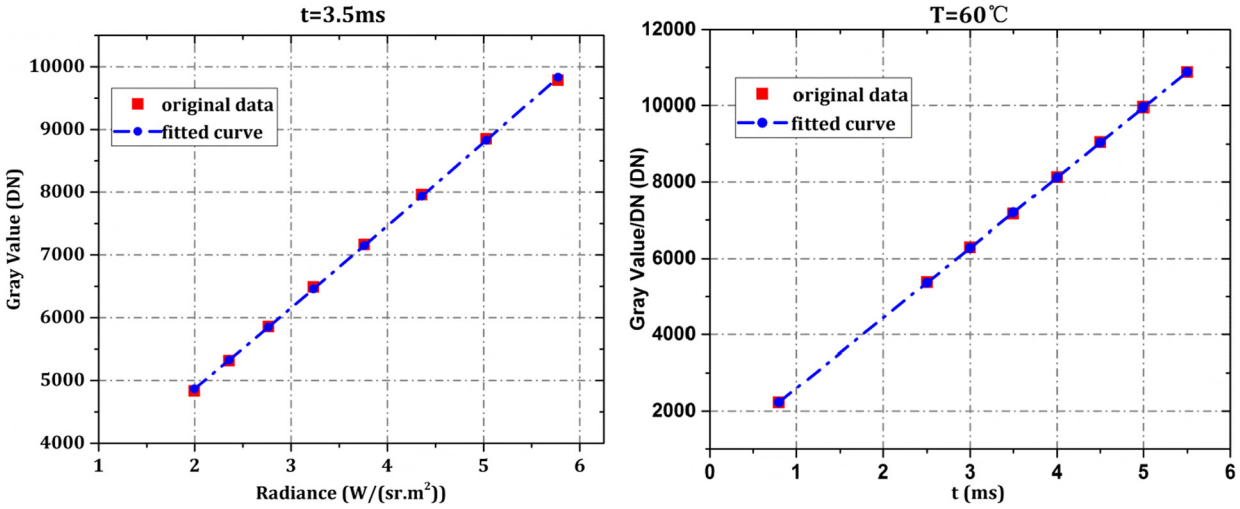

Fig. 3. (a) Relationship between system output and radiance at a fixed integration time 3.5 ms. (b) Relationship between system output and integration time at a fixed temperature 40 °C.

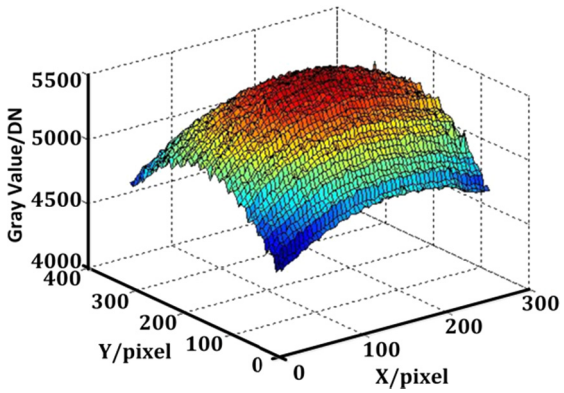

Fig. 4. Raw output signal of an extended area blackbody. The raw image manifests different photo responses of pixels.

calibration was conducted on the infrared system. The ambient temperature was about 15 °C, while the atmospheric pressure was 985.5 hPa and the relative humidity was 58.9%. In Fig. 3 **(a)**, the integration time of 3.5 ms was set and the temperature rose from 40 °C to 75 °C with 5 °C as a step. We can see the gray value was linear to the radiance in Fig. 3(a). At the same time, the temperature of blackbody was fixed at 60 °Cand the integration time was changed from 0.8 ms to 5.5 ms. The relationship between the gray value and the integration time showed a good linear relationship as illustrated in Fig. 3(b). Both of experimental results above proved the effectiveness of the model of wide dynamic calibration considering integration time.

4.3. Results of non-uniformity correction

For an infrared radiometry system, there is serious non-uniformity in raw image as shown in Fig. 4. Generally, the phenomenon of non-uniformity is characterized by stripes emerged and response inconsistent. To remove these effects, NUC is required to conduct. In most cases, the performance of the NUC algorithm is usually quantitatively evaluated a metric that is commonly used in assessing the fixed-pattern noise in infrared image. The metric is the Non-Uniformity parameter NU. It is adopted to assess the images of a uniformity background. The parameter NU is defined below [29,30]:

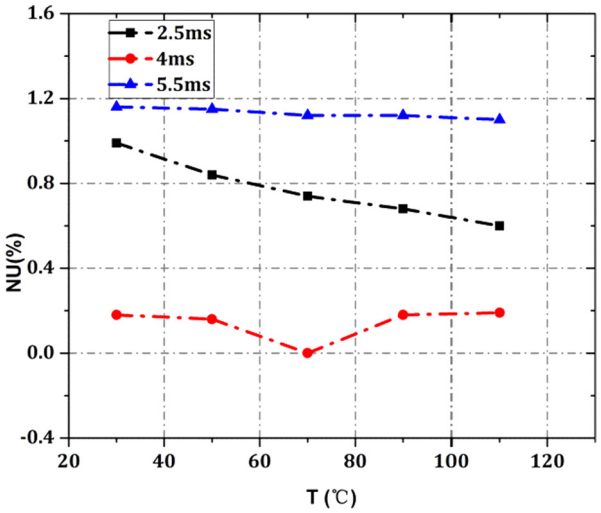

Fig. 5. Result of blackbody-based NUC. Relationship between *NU* and temperature *T* at different integration times referring to 2.5 ms, 4 ms and 5.5 ms.

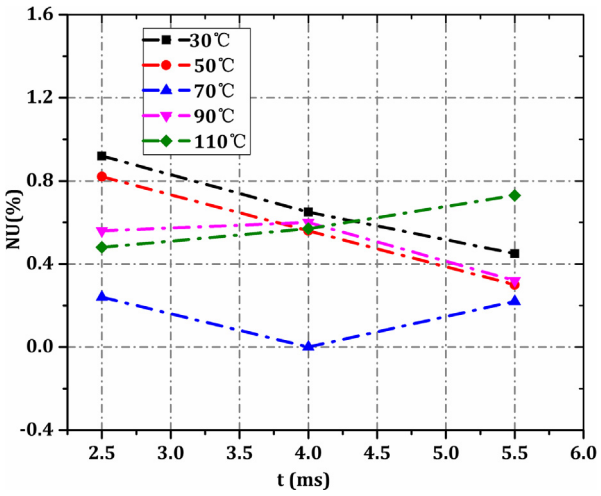

Fig. 6. Result of integration-based NUC. Relationship between *NU* and integration time at different temperatures referring to 30 °C, 50 °C, 70 °C, 90 °Cand 110 °C.

$$\begin{cases} NU = \frac{1}{\bar{I}} \cdot \sqrt{\frac{1}{M \times N - d} \cdot \sum_{i=1}^{M} \sum_{j=1}^{N} (I_{i,j} - \bar{I})^2} \times 100\% \\ \bar{I} = \frac{1}{M \times N - d} \cdot \sum_{i=1}^{M} \sum_{j=1}^{N} I_{i,j} \end{cases}, \quad (23)$$

where $\bar{I}$ is the average gray value of all pixels, but not including bad pixels, $I_{i,j}$ is the gray value of (i,j)th pixel in the array, d is the number of bad pixels. M×N is the number of pixels in infrared focal plane array.

In order to verify the feasibility and validity of high-efficiency NUC method, a series of experiments were done in the outfield. The integration times 2.5 ms, 4 ms, 5.5 ms and the temperatures 30 °C, 50 °C, 70 °C, 90 °C, 110 °C were picked out as the sampling points. Then the raw data was processed by the following methods, namely BBNUC, IBNUC and the proposed high-efficiency NUC, which are illustrated as follows:

(1) For BBNUC method, two different temperatures (60 °Cand 70 °C) and a integration time (4 ms) were chosen to calculate NUC coefficients. After the raw images corrected by BBNUC, the average of NU at different integration times was 0.68%. Since the coefficients of BBNUC were obtained at 4 ms, it was provided with high accuracy approximate 0.14% at 4 ms. However, if the same parameters were still applied to other integration times, it would lead to poor accuracy (0.77% at 2.5 ms and 1.13% at 5.5 ms). The results were shown in Fig. 5. The results indicated that the coefficients of BBNUC acquired at a fixed time are not suitable to operate at other integration times. In other words, the BBNUC method was limited to variable integration time.

(2) For IBNUC method, one temperature (70 °C) and two different integration times (2.5 ms and 4 ms) were chosen to calculate NUC coefficients. After the raw image processed by IBNUC, the average NU was 0.52% at all sampling temperatures. From Fig. 6, we can see that due to the coefficients of IBNUC achieved at 70 °C, a high accurate output was gained at 70 °C about 0.15%. But at other temperature points, the results of NU were deteriorated rapidly (0.68% at 30 °C, 0.56 at 50 °C, 0.5% at 90 °C, 0.59% at 110 °C). Thus, the coefficients of IBNUC obtained at a given temperature point could only be applied to the given temperature. Above all, the IBNUC method was not fit for a WDR and CVIT system.

(3) At the same time, to verify that the high-efficiency NUC method proposed in this paper was no longer restricted to the integration time. The comparisons were conducted between our method and BBNUC method in different integration times. As shown in Fig. 7(a), the two methods have similar accuracy under an integration time of 4 ms (average

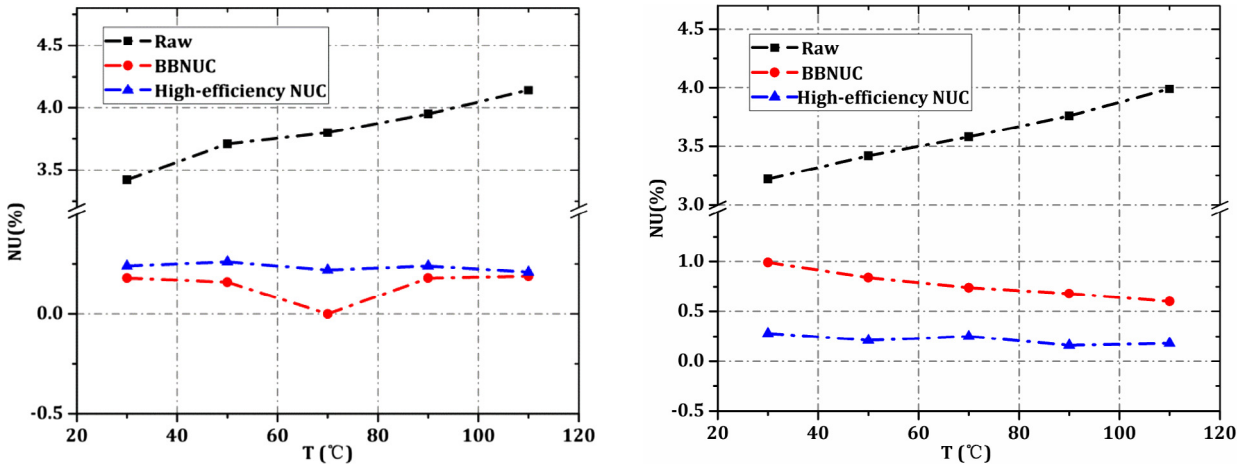

(a) NU results of BBNUC and high-efficiency NUC at 4ms. (b) NU results of BBNUC and high-efficiency NUC at 2.5ms.

Fig. 7. (a) NU results of BBNUC and high-efficiency NUC at 4 ms. (b) NU results of BBNUC and high-efficiency NUC at 2.5 ms.

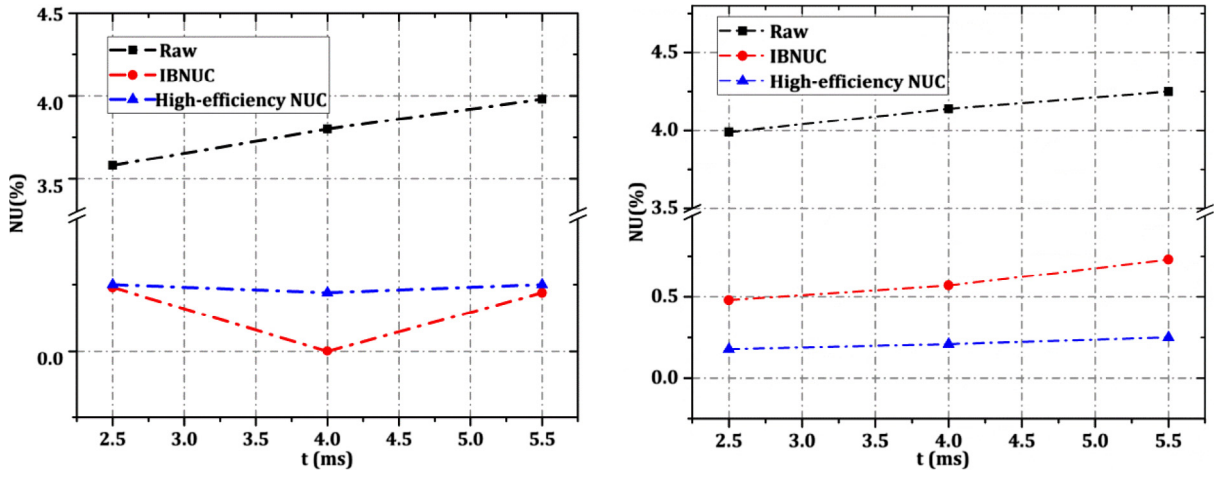

(a) NU results of IBNUC and high-efficiency NUC at 70℃. (b) NU results of IBNUC and high-efficiency NUC at 110℃.

Fig. 8. (a) NU results of IBNUC and high-efficiency NUC at 70 °C. (b) NU results of IBNUC and high-efficiency NUC at 110 °C.

NU of BBNUC was 0.14% and average NU of our high-efficiency NUC was 0.23%). However, effects of the proposed method were better than IBNUC at other integration time such as 2.5 ms (average NU of BBNUC was 0.77% and average NU of high-efficiency NUC was 0.21%), the results were shown clearly in Fig. 7(b). In a word, the effects of high-efficiency NUC showed good stability compared with BBNUC.

Table 1
The data of NUC experiment.

t/ms	T/°C	Raw NU/%	BBNUC NU/%	IBNUC NU/%	High-efficiency NU/%
2.5	30	3.22	0.99	0.92	0.28
	50	3.42	0.84	0.82	0.21
	70	3.58	0.74	0.24	0.25
	90	3.76	0.68	0.56	0.16
	110	3.99	0.60	0.48	0.18
4	30	3.42	0.18	0.65	0.24
	50	3.71	0.16	0.56	0.26
	70	3.80	0	0	0.22
	90	3.95	0.18	0.60	0.24
	110	4.14	0.19	0.57	0.21
5.5	30	3.62	1.16	0.45	0.27
	50	3.81	1.15	0.30	0.26
	70	3.98	1.12	0.22	0.25
	90	4.06	1.12	0.32	0.27
	110	4.25	1.10	0.73	0.25
Average value/%		3.78	0.68	0.49	0.24

Considering the factor of temperature, results of our method and IBNUC method were compared at different temperatures as shown in Fig. 8(a) and (b). As we expect, the accuracy was high at 70 °C with the both methods (average NU of IBNUC was 0.15% and average NU of high-efficiency NUC was 0.24%). However, at 110 °C, our method provided a much better result comparing to IBNUC (average *NU* of IBNUC was 0.60% and average NU of high-efficiency NUC was 0.21%). Similarly, we conducted series of experiments at other temperatures (30 °C, 50 °Cand 90 °C), the results confirmed that our method also surpassed the IBNUC. The non-uniformity correction results of various methods were given in Table 1.

To verify the feasibility of the high-efficiency NUC, the raw images of a scene were obtained at different integration times. The correction coefficients of BBNUC were obtained at 4 ms and applied to a 4 ms scene and a 2.5 ms scene respectively, which were demonstrated in Fig. 9(a) and (b). From the scenes after correction, we can see that changing the integration time would make the NUC results degenerate, which was manifested as the obvious stripe. Fig. 9(a) and (b) are the scenes corrected by the proposed high-efficiency NUC method. We can see that with the integration time switching, the proposed NUC method shows better performance comparing with BBNUC. To sum up, the proposed NUC method in this paper takes both temperature and integration time into account, it's valid for any temperature and random integration time theoretically in the linear region. Hence, the high-efficiency NUC method is suitable for a WDR and CVIT infrared radiometry system.

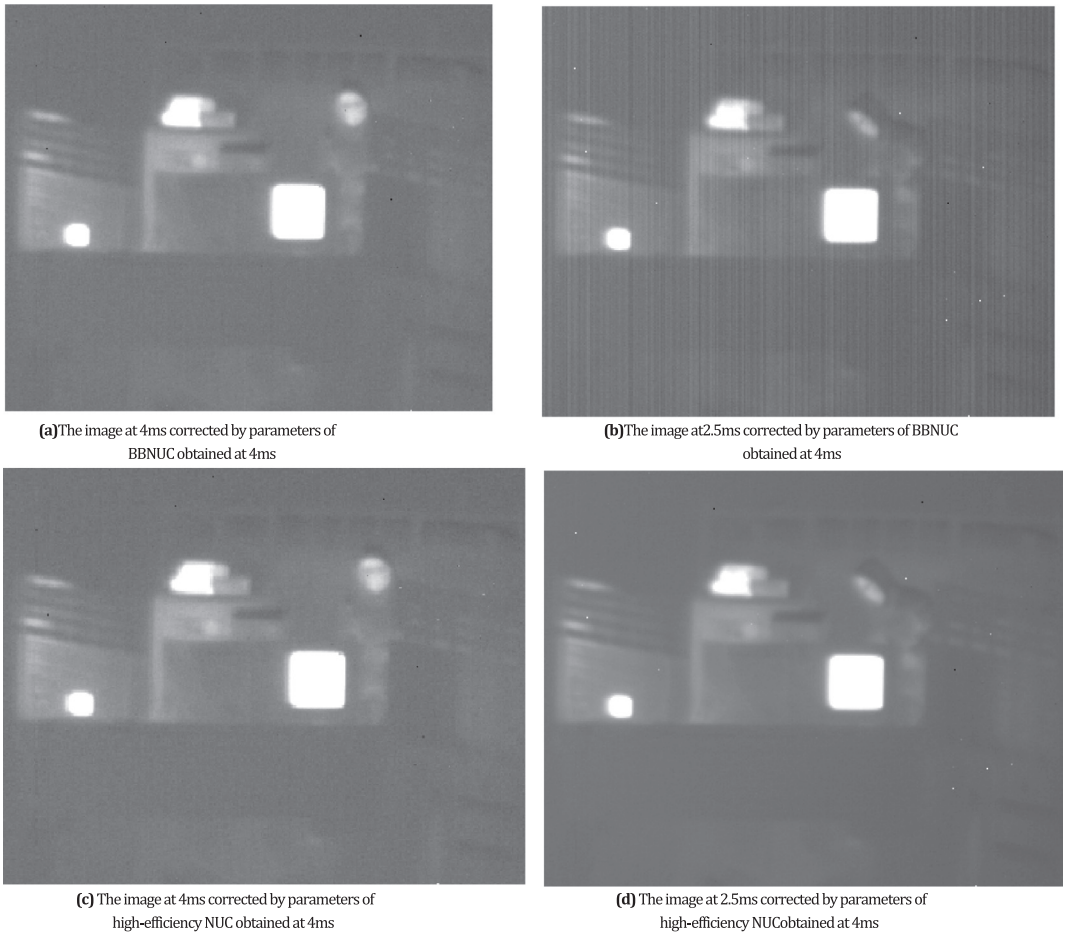

(a) The image at 4ms corrected by parameters of BBNUC obtained at 4ms

(b) The image at2.5ms corrected by parameters of BBNUC obtained at 4ms

(c) The image at 4ms corrected by parameters of high-efficiency NUC obtained at 4ms

(d) The image at 2.5ms corrected by parameters of high-efficiency NUCobtained at 4ms

Fig. 9. NUC results of the high-efficiency NUC and BBNUC for an outfield scene.

5. Conclusion

In summary, we have introduced an effective and time-saving NUC method called high-efficiency NUC. This method derives from the calibration-based non-uniformity correction and takes the factors of integration time and temperature into account in linear region. The greatest advantage of the proposed method is that it obtains the coefficients of NUC for an infrared radiometry system with WDR and CVIT by only three different images. The limitations of traditional methods have been analyzed and the proposed method has been deduced, then experimental verification has been described. Compared with BBNUC, high-efficiency NUC breaks through the constraint of integration time. Meanwhile, compared to the IBNUC, the results of high-efficiency NUC method is obviously more effective for imaging WDR scenes. Since the coefficients of high-efficiency NUC can be obtained by only three different images, it can be used widely in infrared radiometry systems to reduce the workload, simplify the equipment and save the time. What has to be pointed out is that the proposed method is still limited in the theory of linearity. Combined with the multi-point NUC method, which is suitable for nonlinear region, the high-efficiency NUC could be discussed further and a large quantity of experiments should be conducted in the future.

Conflict of interest

The authors declare that there is no conflict of interest.

References

[1] A.F. Milton, F.B. Barone, M.R. Kruer, Influence of nonuniformity on infrared focal plane array performance, Opt. Eng. 24 (1985) 855–862.
[2] W. Zhao, C. Zhang, Scene-based nonuniformity correction and enhancement: pixel statistics and subpixel motion, J. Opt. Soc. Am. 25 (7) (2008) 1668–1681.
[3] D.A. Scribner, M.K. Kruer, J.M. Killiany, Infrared focal plane array technology, Proc. IEEE 79 (1) (1991) 66–85.
[4] J.-H. Kim et al., Regularization approach to scene-based nonuniformity correction, Opt. Eng. 53 (5) (2014) 053105.
[5] Y. Cao, C.L. Tisse, Shutterless solution for simultaneous focal plane array temperature estimation and nonuniformity correction in uncooled long-wave infrared camera, Appl. Opt. 52 (2013) 6266–6271.
[6] D.R. Pipa, E.A. da Silva, C.L. Pagliari, P.S. Diniz, Recursive algorithms for bias and gain nonuniformity correction in infrared videos, IEEE Trans. Image Process 21 (2012) 4758–4769.
[7] M. Ochs, A. Schulz, H.J. Bauer, High dynamic range infrared thermography by pixelwise radiometric self calibration, Infra. Phys. Technol. 53 (2010) 112–119.
[8] M. Frédérick, T. Pierre, F. Vincent, Infrared camera NUC and calibration: comparison of advanced methods, Infra. Imag. Syst. 8706 (2013) 870603-1.
[9] E. Vera, Pablo Meza, Sergio N. Torres, Total variation adaptive scene-based nonuniformity correction, Information Systems, 2010.
[10] X. Sui, Q. Chen, G. Gu, Nonuniformity correction of infrared images based on infrared radiation and working time of thermal imager, Optik – Int. J. Light Electron Opt. 124 (2013) 352–356.
[11] M. Jin, W. Jin, Y. Li, S. Li, An evaluation method based on absolute difference to validate the performance of SBNUC algorithms, Infra. Phys. Technol. 78 (2016) 1–12.
[12] S.H. Rong, H.X. Zhou, H.L. Qin, R. Lai, K. Qian, Nonuniformity correction for an infrared focal plane array based on diamond search block matching, J. Opt. Soc. Am. A Opt. Image Sci. Vis. 33 (2016) 938–946.
[13] Z. Li, T. Shen, S. Lou, Scene-based nonuniformity correction based on bilateral filter with reduced ghosting, Infra. Phys. Technol. 77 (2016) 360–365.
[14] H. Yu, Z.J. Zhang, C.-S. Wang, An improved retina-like nonuniformity correction for infrared focal-plane array, Infra. Phys. Technol. 73 (2015) 62–72.
[15] Z. Liu, Y. Ma, J. Huang, F. Fan, J. Ma, A registration based nonuniformity correction algorithm for infrared line scanner, Infra. Phys. Technol. 76 (2016) 667–675.
[16] Z. Chao, Q. Chen, G.H. Gu, X.B. Sui, Scene-based nonuniformity correction algorithm based on interframe registration, Opt. Soc. Am. 28 (2011) 1164–1176.
[17] W. Qian, Q. Chen, J. Baiand, G. Guo, Adaptive convergence nonuniformity correction algorithm, Appl. Opt. 50 (2011) 1–10.
[18] J. Zhao, Q. Zhou, Y. Chen, T. Liu, H. Feng, Z. Xu, Q. Li, Single image stripe nonuniformity correction with gradient-constrained optimization model for infrared focal plane arrays, Opt. Commun. 296 (2013) 47–52.
[19] B. Gutschwager, J. Hollandt, Nonuniformity correction of imaging systems with a spatially nonhomogeneous radiation source, Appl. Opt. 54 (2015) 10599–10605.
[20] Z.Y. Sun, S.T. Chang, W. Zhu, Radiometric calibration method for large aperture infrared system with broad dynamic range, Appl. Opt. 54 (2015) 4659–4666.
[21] R.H. Yang, J. Zhang, H.X. Deng, et al., A Calibration Technology for Multi-camera System with Various Focal Lengths, Proc. SPIE9903, 99032S, 2016.
[22] S. Kim, Two-point correction and minimum filter-based nonuniformity correction forscan-based aerial infrared cameras, Opt. Eng. 51 (10) (2012) 106401–106411.
[23] M. Vollmer, K.P. Mollmann, Infrared thermal imaging fundamentals, research and applications, Wiley-VCH Verlag GmbH & Co, K Ga A, 2010.
[24] S.T. Chang, Z.X.Y. Zhang, S.Z.Y. Sun, M. Li, Method to remove the effect of ambient temperature on radiometric calibration, Appl. Opt. 53 (2014) 6274–6279.
[25] L.J. Huo, D. Zhou, D. Wang, R. Liu, B. He, Staircase-scene-based nonuniformity correction in aerial point target detection systems, Appl. Opt. 55 (2016) 7149–7156.
[26] P.W. Nugent, J.A. Shaw, N.J. Pust, Radiometric calibration of infrared imagers using an internal shutter as an equivalent external blackbody, Opt. Eng. 53 (2014) 123106.
[27] A.E. Mudau, C.J. Willers, D. Griffith, F.P.J. le Roux, Non-uniformity correction and bad pixel replacement on LWIR and MWIR images, in: Conference: Electronics, Communications and Photonics Conference, 2011, pp. 1–5.
[28] P. David, Linear theory of nonuniformity correction in infrared staring sensors, Opt. Eng. 32 (1993).
[29] H.-X. Zhou, H.-L. Qin, R. Lai, B.-J. Wang, L.-P. Bai, Nonuniformity correction algorithm based on adaptive filter for infrared focal plane arrays, Infra. Phys. Technol. 53 (2010) 295–299.
[30] Shanghai Institute of Technical Physics of Chinese Academy of Sciences, GB/T 17444-4988, The technical norms of measurement and test of characteristic parameters of infrared focal plane arrays, China Zhijian Publishing House, Beijing, 1980 (in Chinese).